Abrupt climate transition of icy worlds from snowball to moist or runaway greenhouse

Jun Yang[1]*, Feng Ding[2], Ramses M. Ramirez[3], W. R. Peltier[4], Yongyun Hu[1]* and Yonggang Liu[1]

Ongoing and future space missions aim to identify potentially habitable planets in our Solar System and beyond. Planetary habitability is determined not only by a planet's current stellar insolation and atmospheric properties, but also by the evolutionary history of its climate. It has been suggested that icy planets and moons become habitable after their initial ice shield melts as their host stars brighten. Here we show from global climate model simulations that a habitable state is not achieved in the climatic evolution of those icy planets and moons that possess an inactive carbonate–silicate cycle and low concentrations of greenhouse gases. Examples for such planetary bodies are the icy moons Europa and Enceladus, and certain icy exoplanets orbiting G and F stars. We find that the stellar fluxes that are required to overcome a planet's initial snowball state are so large that they lead to significant water loss and preclude a habitable planet. Specifically, they exceed the moist greenhouse limit, at which water vapour accumulates at high altitudes where it can readily escape, or the runaway greenhouse limit, at which the strength of the greenhouse increases until the oceans boil away. We suggest that some icy planetary bodies may transition directly to a moist or runaway greenhouse without passing through a habitable Earth-like state.

Icy worlds are common in the Solar System (such as Europa[1], Enceladus[2], Ganymede[3] and early Earth[4]) and plausibly also in extrasolar systems[5]. A fundamental question is: would such icy planets and moons become habitable once their ice cover melts? There are two ways for the icy worlds to escape the globally ice-covered snowball states. One is that continuous atmospheric accumulation of CO_2 from volcanic outgassing during the snowball phase triggers the melting[6,7]; this is plausible for planets having an active carbon cycle (for example, Earth), and they become habitable for life after the ice melts. The other is that the stars brighten with time and the ice melts once the stellar flux exceeds a critical value[8]; this is the case for planets and moons lacking an active carbon–silicate cycle and having low concentrations of greenhouse gases (for example, Europa). Here, we investigate the second case using a series of three-dimensional (3D) climate model experiments. In contrast to previous studies[9–11] that suggest the existence of a habitable world after the snowball deglaciation, we show that the increased stellar insolation will force the planet into an uninhabitable moist or even runaway greenhouse state.

Using 0D and 1D energy balance climate models and a 3D grey-gas atmospheric general circulation model (GCM), previous studies[12–14] had examined the climate evolution of a snowball planet having low concentrations of greenhouse gases. However, their models were unable to account for the effects of clouds, lapse rate, spatial snow and ice distributions, realistic atmospheric radiative transfer, and/or meridional atmospheric heat transport, which have been identified[15,16] to be critical for simulating the snowball climate. Moreover, the simple climate models cannot simulate vertical water vapour transports or the onset of a moist greenhouse state. These studies[12–14] showed that a post-snowball climate should be hot, but whether it is habitable for life or not remains unclear.

First, we calculate the stellar flux threshold required to trigger the melting of a snowball planet orbiting different types of star (from F to K), using the 3D global GCM CAM3 (see Methods).

Model comparisons[17–19] had demonstrated that CAM3 could accurately simulate a snowball Earth climate that possibly occurred 600–800 million years ago. In the second step, we fix the insolation at the stellar flux threshold and allow the ice to melt, to examine whether the post-snowball planet will fall into a moist or runaway greenhouse state. The moist greenhouse state is defined as that in which water vapour concentration in the upper atmosphere is high enough that H_2O photo-dissociation and subsequent H escape to the space becomes significant[8,20]. When the water vapour mixing ratio reaches 3×10^{-3}, a planet having an equivalent water inventory to Earth's would lose all of the water within the present-day age of the Solar System, 4.5 billion years[8]. The runaway greenhouse state is defined as that in which the atmosphere becomes optically thick at all infrared wavelengths due to the water vapour greenhouse effect, absorbed stellar flux exceeds allowed maximum outgoing longwave radiation, and surface liquid water evaporates entirely into the atmosphere[12,21]. These two climate states constrain the inner edge of surface liquid water habitable zone[8].

Stellar flux threshold for snowball melting

For a solar spectrum, a fixed CO_2 concentration of 300 ppmv (that is, close to the pre-industrial level), an ice albedo of 0.5 (the typical albedo of sea ice on Earth[22]) and a snow albedo of 0.8, the stellar flux required to trigger the snowball melting is 1,800 W m^{-2} (Fig. 1), which is 32% higher than the solar flux for the modern Earth. In the snowball state, the surface is cold, mainly because the surface albedo is high[12,13] and the greenhouse effect is weak (4–14 K in global mean, versus 33 K for Earth) due to low water vapour concentration[15]. For instance, in the case of a solar flux of 1,400 W m^{-2}, the planetary albedo is 0.71 (Europa's albedo is ~0.62 (ref. 1) and Enceladus's ~0.90 (ref. 2)), the vertically integrated water vapour amount is only 0.2 kg m^{-2} (or 1% of modern Earth's), and the global-mean surface temperature is only 214 K. As the stellar flux is increased, the climate sensitivity is 0.2–0.8 K per W m^{-2}, much lower than that

[1]Laboratory for Climate and Atmosphere-Ocean Studies, Department of Atmospheric and Oceanic Sciences, School of Physics, Peking University, Beijing 100871, China. [2]Department of the Geophysical Sciences, University of Chicago, Chicago, Illinois 60637, USA. [3]Carl Sagan Institute, Department of Astronomy, Cornell University, Ithaca, New York 14853, USA. [4]Department of Physics, University of Toronto, Ontario M5S 1A7, Canada.
*e-mail: junyang@pku.edu.cn; yyhu@pku.edu.cn
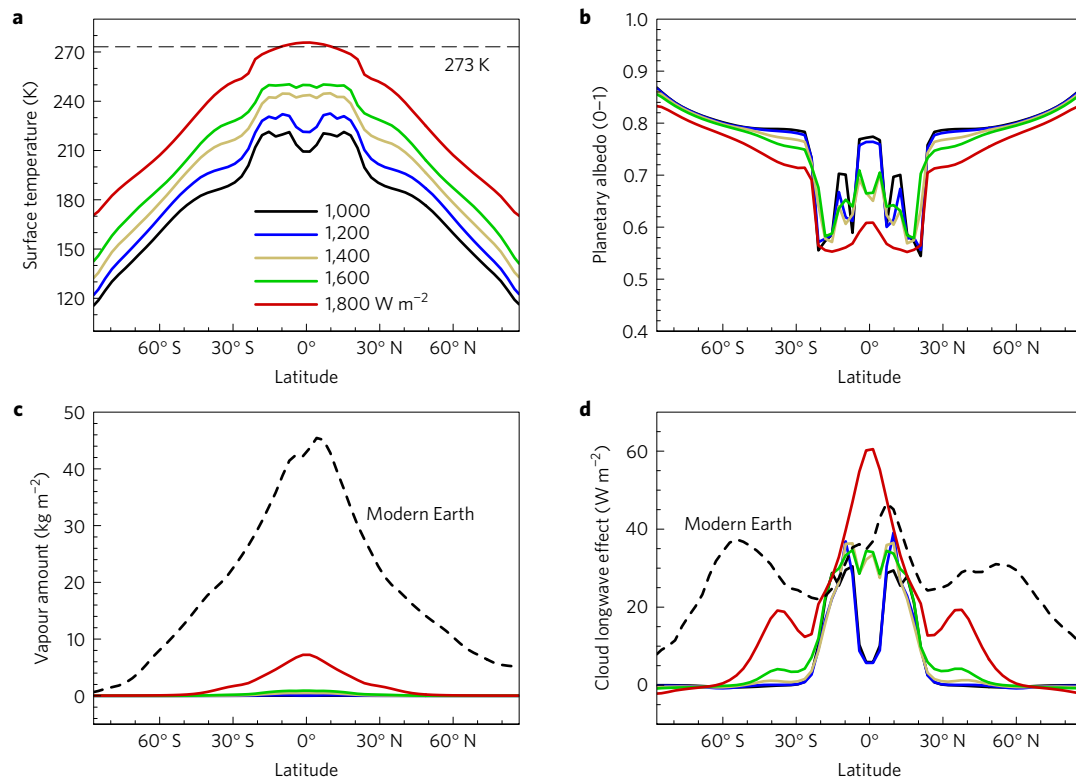
Figure 1 | Climates of a snowball planet around a G star. a–d, Annual- and zonal-mean surface temperature (**a**), planetary albedo (**b**), vertically integrated water vapour amount (**c**) and cloud longwave radiation effect at the top of the model (**d**). Stellar fluxes are 1,000, 1,200, 1,400, 1,600 and 1,800 W m^{-2}. The horizontal dashed line in **a** is the melting point (273 K), and the dashed lines in **c**,**d** are the corresponding values for the modern Earth. In these cases, ice albedo is 0.5, snow albedo is 0.8, CO_2 amount is 300 ppmv and obliquity is 0°.

of the modern Earth[23], 0.7–1.9 K per W m^{-2}. Clouds have a small shortwave cooling effect due to the masking of the high surface albedo and a moderate longwave warming effect (7–20 W m^{-2} in global mean). In the region around 15° S(N), the planetary albedo is lower than that in other latitudes (Fig. 1b), which is due to the fact that there is nearly no snow over ice in this region where sublimation is stronger than snowfall. When the surface is set to have a surface albedo of 0.6 everywhere (that of sea glacier, which is compressed thick snow overlying ocean[24]), the stellar flux threshold is still high, 1,600 W m^{-2} (Supplementary Fig. 1).

Sensitivity tests show that the stellar flux threshold is around 1,500–1,900 W m^{-2} for a wide range of parameters, including ice cloud particle size, planetary obliquity, eccentricity, gravity, radius, background gas concentration (N$_2$) and surface topographic height (Fig. 2a). The robustness of our conclusion is due to the simplicity of the mechanism: any planet that has a high albedo and a low greenhouse gas concentration should have low surface temperature and thereby require a high stellar flux to trigger the melting. When the gravity and radius are set to those of Europa, the stellar flux threshold is still high, 1,550–1,600 W m^{-2}. Increasing the N$_2$ partial pressure from 1 to 10 bars has a small (<3 K) effect on the maximum surface temperature and thereby nearly does not affect the stellar flux threshold. This is due to the compensation between the warming effect through increasing pressure broadening and the cooling effect via enhancing Rayleigh scattering and increasing equator-to-pole atmospheric heat transport (Supplementary Fig. 2). Increasing the obliquity from 0° to 30° raises the stellar flux threshold by 100–300 W m^{-2} (depending on the surface albedo), primarily due to the fact that less solar energy is deposited at the equator, where the annual-mean surface temperature is the maximum. Halving or doubling ice cloud particle sizes has a very small effect (<50 W m^{-2}) on the result.

Compared with a G-star spectrum, the stellar flux threshold for an F-star spectrum is higher, 1,700–2,200 W m^{-2} (Fig. 2b). This is due to a blueshift of the spectrum[8] and therefore a higher surface albedo[25]. For a K-star spectrum, the stellar flux threshold is lower, 1,150–1,300 W m^{-2} (Fig. 2c), due to the redder spectrum. For G- and F-star systems, the stellar flux thresholds are close to or even higher than both the moist[26–28] and runaway[29–31] greenhouse limits (Fig. 2a). Exceptions are that for slowly rotating planets[26], synchronously rotating planets around M stars[32], and desert planets with limited surface water[33], their moist and runaway greenhouse limits could be higher than the stellar flux thresholds found here.

Transition to a moist or runaway greenhouse state

For a G- or F-star system, when the stellar flux deposited on an icy planet reaches the snowball-melting stellar flux threshold, surface ice melts completely and the atmosphere enters into a moist greenhouse state. After the ice melts, surface albedo decreases from 0.5–0.8 to as low as 0.09, total water vapour amount reaches >500 kg m^{-2} (implying a strong greenhouse effect), and upper-atmospheric water vapour concentration becomes higher than the moist greenhouse level of 3×10^{-3} (Fig. 3 and Supplementary Fig. 3). Energy balance analyses (Fig. 3e) suggest that equilibrium surface temperatures would be 7–19 K higher (for the G-star case, assuming the climate sensitivity[23] is 0.7–1.9 K per W m^{-2}) and 35–95 K higher (for the F-star case) than the last converged solutions shown in the figure, if the model could be integrated longer. Decreasing cloud particle size, increasing planetary radius, or reducing gravity makes the planet enter a moist greenhouse state at lower stellar fluxes, and vice versa (Supplementary Figs 4 and 5). The most sensitive parameter is the gravity, due to the fact that low gravity decreases atmospheric effective emission pressure and temperature[12].
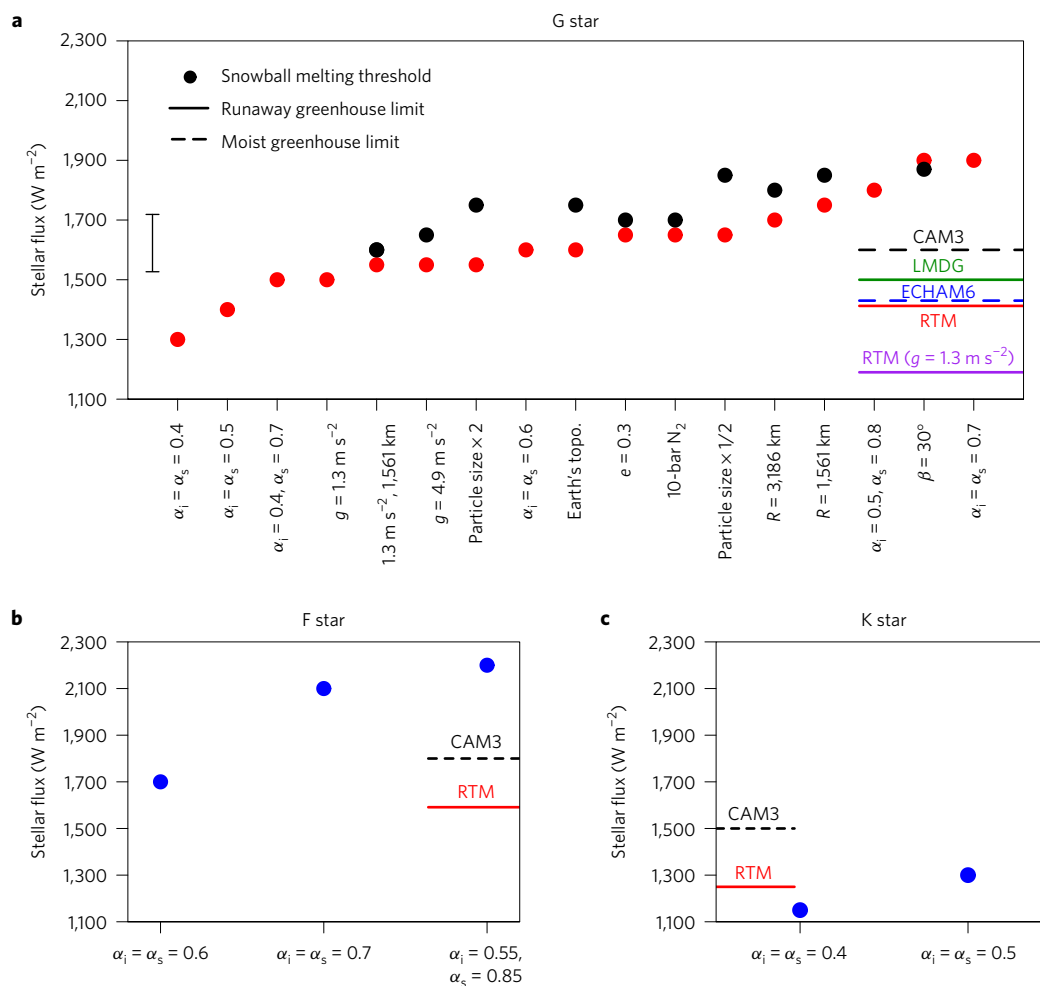
Figure 2 | Comparison between snowball melting threshold and moist or runaway greenhouse limit. a–c, Stellar flux thresholds for melting snowballs around G (**a**), F (**b**) and K (**c**) stars. Horizontal dashed and solid lines are the moist and runaway greenhouse limits, respectively, obtained by the 3D GCM CAM3 (ref. 26), CAM4_Wolf[27], ECHAM6 (ref. 28), LMDG[29] and 1D radiative-transfer model (RTM)[30,31]. The vertical bar in **a** is the uncertainty range (170 W m^{-2}, see Methods). Sensitivity parameters include ice albedo (α_i), snow albedo (α_s), gravity (g), radius (R), eccentricity (e), obliquity (β), ice cloud particle size, topographic height and N$_2$ partial pressure. $\alpha_i = \alpha_s = 0.6$ (red dots), $\alpha_i = 0.5$ and $\alpha_s = 0.8$ (black dots), except if mentioned otherwise.

In the G- and F-star experiments, absorbed stellar radiation is higher than allowed maximum outgoing longwave radiation (Fig. 3f). These planets, therefore, would be expected to enter runaway greenhouse states, in which surface temperature would keep increasing to above 1,400 K (ref. 8), at which point the surface begins to radiate in the visible wavelengths to balance the excess stellar energy. In the K-star experiment, the ice line retreats to 50° S(N) and the post-snowball surface temperature, 284 K in global mean (Fig. 3b), is similar to the modern Earth's. This is due to the redder spectrum and thereby a lower surface albedo and a lower snowball-melting stellar flux threshold.

The snowball-melting stellar flux threshold is sensitive to surface albedo, and the runaway greenhouse limit depends on gravity. If surface ice were mixed with dust, surface albedo would be low, which can decrease the stellar flux threshold significantly. For a dirty ice surface having an albedo of 0.4, the threshold is only 1,300 W m^{-2} (Fig. 2a). This threshold is lower than the moist and runaway greenhouse limits for Earth-gravity planets; however, it is still high enough to trigger a runaway greenhouse state on moons that have low gravity. For a moon with gravity of 1.3 m s^{-2} (Europa's), the allowed maximum outgoing longwave radiation[12] is only 238 W m^{-2} and the runaway greenhouse limit is 1,190 W m^{-2} (if assuming the post-snowball planetary albedo is 0.2).

Implications for planetary evolution

Our results suggest that an icy exoplanet at the equivalent distance of the modern Earth from the Sun would remain in a snowball state for 10^9 years or even longer until its received stellar flux evolves to become much higher than the insolation for the modern Earth. Following this, the planet would directly jump to a moist or runaway greenhouse state (Fig. 4). Europa and Enceladus will have no habitable period. They will transit to a moist or runaway greenhouse state when the Sun becomes a red giant in 6–7 billion years, at which time the stellar flux at the location of Europa will reach the snowball-melting threshold. Our results also suggest that a globally frozen planet can remain not only near the outer edge of the liquid water habitable zone[5,34,35] but also near the inner edge or even further inward, especially in F- and G-star systems. Some exoplanets that were thought to be potentially habitable or to be in a runaway greenhouse state (such as Kepler-22b (ref. 36) around a G star, which receives ∼1.1 times Earth's insolation) may actually remain in snowball states if they started with globally ice-covered oceans (that is, the so-called 'cold start'[8]).

Finally, we emphasize that our conclusion applies to planets that have an inactive carbonate–silicate cycle and low concentrations of greenhouse gases in G-star and F-star systems. Compared with Earth-mass planets, smaller planets and moons are more likely at risk of the abrupt climate transition because they
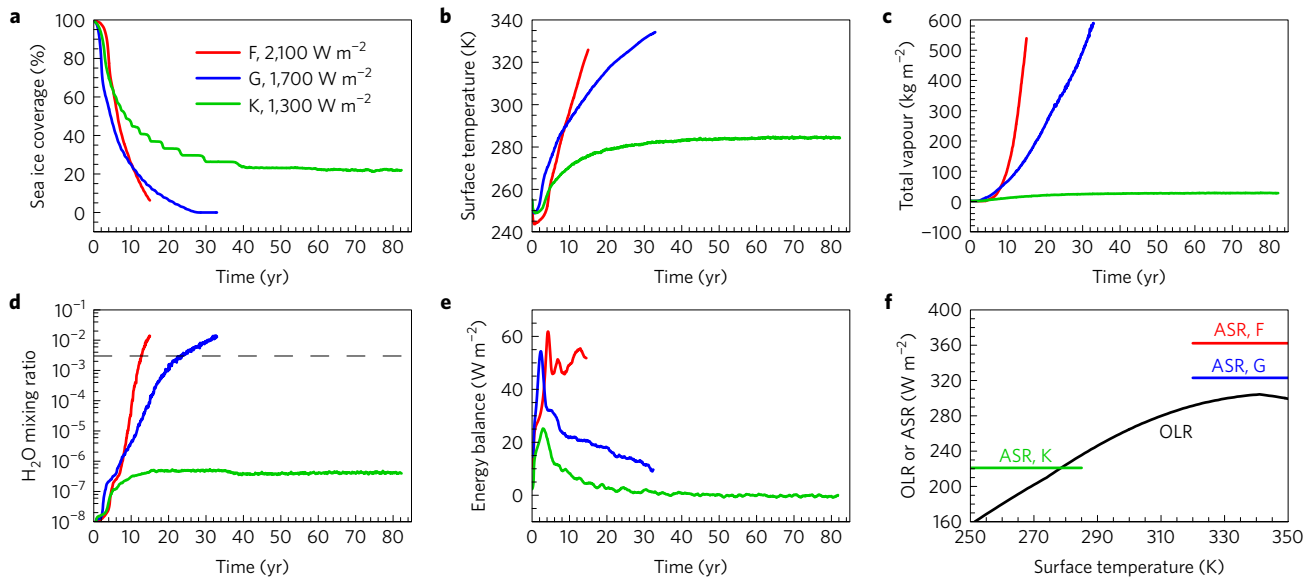
Figure 3 | Climate evolution of snowball planets. a–e, Global-mean ice coverage (**a**), surface temperature (**b**), vertically integrated water vapour amount (**c**), vapour volume mixing ratio at 50 hPa (**d**) and energy balance (**e**, absorbed shortwave radiation (ASR) minus outgoing longwave radiation (OLR)), as a function of time. **f**, OLR as a function of surface temperature (black line, see Methods) and ASR from the last converged solutions of the experiments (horizontal lines). Red line, 2,100 W m^{-2} and F star; blue, 1,700 and G star; and green, 1,300 and K star. In **d**, the dashed line is the critical moist greenhouse level.
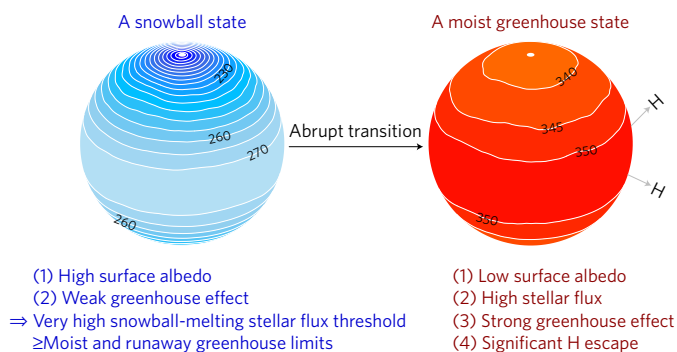
Figure 4 | Schematic illustration of the climate transition under stellar brightening and the underlying physical mechanisms. The climate transition from a snowball state to a moist greenhouse state (or even a runaway greenhouse state) is abrupt, dramatic and irreversible. The contour lines are surface temperatures right before the snowball melting (left) and after the snowball melting (right), with a contour interval of 5 K.

Methods

Methods, including statements of data availability and any associated accession codes and references, are available in the online version of this paper.

References

1. Buratti, B. & Veverka, J. Voyager photometry of Europa. *Icarus* **55**, 93–110 (1983).
2. Howett, C. J. A., Spencer, J. R., Pearl, J. & Segura, M. Thermal inertia and bolometric bond albedo values for Mimas, Enceladus, Tethys, Dione, Rhea and Iapetus as derived from Cassini/CIRS measurements. *Icarus* **206**, 573–593 (2010).
3. Showman, A. P. & Malhotra, R. The Galilean satellites. *Science* **286**, 77–84 (1999).
4. Hoffman, P. F., Kaufman, A. J., Halverson, G. P. & Schrag, D. P. A Neoproterozoic snowball Earth. *Science* **281**, 1342–1346 (1998).
5. Tajika, E. Snowball planets as a possible type of water-rich terrestrial planets in the extrasolar planetary system. *Astrophys. J. Lett.* **680**, L53 (2008).
6. Walker, J. C. G., Hays, P. B. & Kasting, J. F. A negative feedback mechanism for the long-term stabilization of Earth's surface temperature. *J. Geophys. Res.* **86**, 9776–9782 (1981).
7. Menou, K. Climate stability of habitable Earth-like planets. *Earth Planet Sci. Lett.* **429**, 20–24 (2015).
8. Kasting, J. F., Whitmire, D. P. & Reynolds, R. T. Habitable zones around main sequence stars. *Icarus* **101**, 108–128 (1993).
9. Shields, A. L., Bitz, C. M., Meadows, V. S., Joshi, M. M. & Robinson, T. D. Spectrum-driven planetary deglaciation due to increases in stellar luminosity. *Astrophys. J. Lett.* **785**, L9 (2014).
10. Ramirez, R. M. & Kaltenegger, L. Habitable zones of post-main sequence stars. *Astrophys. J.* **823**, 1–16 (2016).
11. Wolf, E. T., Shields, A. L., Kopparapu, R. K., Haqq-Misra, J. & Toon, O. B. Constraints on climate and habitability for earth-like exoplanets determined from a general circulation model. *Astrophys. J.* **837**, 1–11 (2017).
12. Pierrehumbert, R. T. *Principles of Planetary Climate* (Cambridge Univ. Press, 2010).
13. North, G. R. Analytical solution to a simple climate model with diffusive heat transport. *J. Atmos. Sci.* **32**, 1301–1307 (1975).
14. Ishiwatari, M., Nakajima, K., Takehiro, S. & Hayashi, Y.-Y. Dependence of climate states of gray atmosphere on solar constant: from the runaway greenhouse to the snowball states. *J. Geophys. Res.* **112**, D13120 (2007).

(1) High surface albedo
(2) Weak greenhouse effect
⇒ Very high snowball-melting stellar flux threshold
  ≥Moist and runaway greenhouse limits

A snowball state

Abrupt transition

A moist greenhouse state

(1) Low surface albedo
(2) High stellar flux
(3) Strong greenhouse effect
(4) Significant H escape

lose their interior heat faster and volcanic outgassing would cease earlier[37]. An exoplanet more massive than Earth may also be at risk if its lithosphere is in the stagnant lid regime like on Venus and Mars[38,39]. Our conclusion, however, does not apply to Earth or Earth-like planets that have an active carbonate–silicate cycle. When CO_2 concentration is higher, the planet would require a smaller stellar flux to trigger the melting due to the CO_2 greenhouse effect (Supplementary Fig. 6). Under a solar flux of 94% of the present level during the Neoproterozoic era 600–800 million years ago, the CO_2 concentration required to melt the snowball Earth is >100,000 ppmv (refs 15,17,18). The post-snowball Earth is hot, but it is in neither a runaway nor a moist greenhouse state (Supplementary Figs 7–9). This is because the solar flux is much lower than the runaway greenhouse limit and the high level of CO_2 acts to cool the upper atmosphere and thereby decrease the H_2O concentration there[40].

15. Pierrehumbert, R. T. High levels of atmospheric carbon dioxide necessary for the termination of global glaciation. *Nature* **429,** 646–649 (2004).
16. Pierrehumbert, R. T., Abbot, D. S., Voigt, A. & Koll, D. D. B. Climate of the Neoproterozoic. *Annu. Rev. Earth Planet. Sci.* **39,** 417–460 (2011).
17. Hu, Y., Yang, J., Ding, F. & Peltier, W. R. Model dependence of the CO_2 threshold for melting the hard snowball Earth. *Clim. Past* **7,** 17–25 (2011).
18. Abbot, D. S. *et al.* Clouds and snowball Earth deglaciation. *Geophys. Res. Lett.* **39,** L20711 (2012).
19. Abbot, D. S. Resolved snowball Earth clouds. *J. Clim.* **27,** 4391–4402 (2014).
20. Kasting, J. F., Chen, H. & Kopparapu, R. K. Stratospheric temperatures and water loss from moist greenhouse atmospheres of Earth-like planets. *Astrophys. J. Lett.* **813,** L3 (2015).
21. Ingersoll, A. P. The runaway greenhouse: a history of water on Venus. *J. Atmos. Sci.* **26,** 1191–1198 (1969).
22. Brandt, R. E., Warren, S. G., Worby, A. P. & Grenfell, T. C. Surface albedo of the Antarctic sea ice zone. *J. Clim.* **18,** 3606–3622 (2005).
23. Meinshausen, M. *et al.* Greenhouse-gas emission targets for limiting global warming to 2 °C. *Nature* **458,** 1158–1162 (2009).
24. Warren, S. G., Brandt, R. E., Grenfell, T. C. & Mckay, C. P. Snowball Earth: ice thickness on the tropical ocean. *J. Geophys. Res.* **107,** 31-1–31-18 (2002).
25. Shields, A. L. *et al.* The effect of host star spectral energy distribution and ice-albedo feedback on the climate of extrasolar planets. *Astrobiology* **13,** 715–739 (2013).
26. Yang, J., Boue, G., Frabrycky, D. C. & Abbot, D. S. Strong dependence of the inner edge of the habitable zone on planetary rotation rate. *Astrophys. J. Lett.* **787,** L2 (2014).
27. Wolf, E. T. & Toon, O. B. The evolution of habitable climates under the brightening Sun. *J. Geophys. Res.* **120,** 5775–5794 (2015).
28. Popp, M., Schmidt, H. & Marotzke, J. Transition to a moist greenhouse with CO_2 and solar forcing. *Nat. Commun.* **7,** 10627 (2016).
29. Leconte, J., Forget, F., Charnay, B., Wordsworth, R. & Pottier, A. Increased insolation threshold for runaway greenhouse processes on Earth-like planets. *Nature* **504,** 268–271 (2013).
30. Kopparapu, R. K. *et al.* Habitable zones around main sequence stars: new estimates. *Astrophys. J.* **787,** 1–6 (2013).
31. Goldblatt, C., Robinson, T. D., Zahnle, K. J. & Crisp, D. Low simulated radiation limit for runaway greenhouse climates. *Nat. Geosci.* **6,** 661–667 (2013).
32. Yang, J., Cowan, N. B. & Abbot, D. S. Stabilizing cloud feedback dramatically expands the habitable zone of tidally locked planets. *Astrophys. J.* **771,** L45 (2013).
33. Abe, Y., Abe-Ouchi, A., Sleep, N. H. & Zahnle, K. J. Habitable zone limits for dry planets. *Astrobiology* **11,** 443–460 (2011).
34. Kasting, J. F. & Harman, C. E. Extrasolar planets: inner edge of the habitable zone. *Nature* **504,** 221–223 (2013).
35. Silva, L., Vladilo, G., Schulte, P. M., Murante, G. & Provenzale, A. From climate models to planetary habitability: temperature constraints for complex life. *Int. J. Astrobiol.* **16,** 244–265 (2016).
36. Borucki, W. J. *et al.* Kepler-22b: a 2.4 Earth-radius planet in the habitable zone of a Sun-like star. *Astrophys. J.* **745,** 1–12 (2012).
37. Kite, E., Manga, M. & Gaidos, E. Geodynamics and rate of volcanism on massive Earth-like planets. *Astrophys. J.* **700,** 1732–1749 (2009).
38. O'Neill, C. & Lenardic, A. Geological consequences of super-sized Earths. *Geophys. Res. Lett.* **34,** L19204 (2007).
39. Miyagoshi, T., Kameyama, M. & Ogawa, M. Thermal convection and the convective regime diagram in super-Earths. *J. Geophys. Res.* **120,** 1267–1278 (2015).
40. Wordsworth, R. & Pierrehumbert, R. T. Water loss from terrestrial planets with CO_2-rich atmospheres. *Astrophys. J.* **778,** 1–19 (2013).

Author contributions

J.Y. led this work. J.Y., F.D. and Y.H. designed the study. J.Y. performed, analysed and interpreted the simulations. F.D., R.M.R., W.R.P., Y.H. and Y.L. assisted with the analysis and interpretation of the data. W.R.P. provided computer code necessary for the simulations. All authors discussed the results and wrote the paper.

Additional information

Supplementary information is available in the online version of the paper. Reprints and permissions information is available online at www.nature.com/reprints. Publisher's note: Springer Nature remains neutral with regard to jurisdictional claims in published maps and institutional affiliations. Correspondence and requests for materials should be addressed to J.Y. or Y.H.

Competing financial interests

The authors declare no competing financial interests.

Methods

Climate model employed. We employ the 3D Community Atmospheric Model version 3, CAM3 (ref. 41). The model solves the primitive equations for atmospheric motion on a rotating sphere and the parameterized equations for radiative transfer, convection, condensation, precipitation, clouds and boundary turbulence[42]. The model has a spectral Eulerian core, a horizontal grid with a resolution of 2.8°, and 26 vertical levels from the surface to the middle stratosphere (3 hPa, that is, ~46 km in altitude when the surface temperature is 330 K). A modified version of the model, in which the number of the vertical levels is increased to 34 and the pressure at the top of the model is extended to 0.2 hPa (that is, ~69 km in altitude when the surface temperature is 330 K), has also been employed (see Supplementary Fig. 3c).

Finding the snow-melting stellar flux threshold. To find the stellar flux threshold for melting a snowball planet, stellar flux at the substellar point is specified as a series of values from 800 W m^{-2} to a critical level in which the maximum annual-mean surface temperature reaches 273 K. The concentrations of atmospheric greenhouse gases (CO_2, CH_4 and N_2O) are fixed. An Earth-like atmosphere is employed, except if mentioned otherwise. Many parameters have also been examined, including ice and snow albedos, eccentricity, obliquity, gravity, radius, ice cloud particle size, surface topographic height (note surface albedo is set to being the same for different heights) and background gas concentration (N_2) (see Supplementary Table 1). Note that in a snowball state, the spatial distribution of snow and bare ice depends on the strength of the seasonal cycle[43] and therefore on the planetary obliquity. Sensitivity tests show that our conclusion is robust in varying the obliquity (Fig. 2a). When the gravity or N_2 partial pressure is changed, the absolute masses (rather than mixing ratio) of CO_2, CH_4 and N_2O are fixed. The snowball state is initialized with a surface temperature of 250 K everywhere, the time step in the model is 900 s, and each experiment is integrated for 20–40 model years.

Comparing with Shields *et al.*[9], the snowball-melting stellar flux threshold found in this study is higher, mainly because of two facts. First, the vertical resolution of the ice module used in Shields *et al.* is too low to resolve diurnal and seasonal cycles (see Figures 1–3 in ref. 44). This induces unrealistic ice melting during midday but no night-time refreezing, termed a 'melt-ratchet effect'[16,44]. In our simulations, we set the surface to be glacial ice[45] (similar to that of Greenland in modern simulations) rather than sea ice[46]. The glacial ice is represented as ten vertical layers, and its resolution is much finer than that of sea ice, which is thereby able to avoid the melt-ratchet effect. Second, the ice and snow albedos used in Shields *et al.* are probably lower than should be in a snowball state. Shields *et al.* employed the sea ice and snow albedos on Earth's polar regions, which are inappropriate for simulating the ice in the cold, dry snowball state—a fundamentally different climatic regime[47–49]. For example, Shields *et al.* used a sea ice albedo of 0.48 under the solar spectrum, which is lower than the suggested sea glacier albedo for snowball climate simulations, 0.55–0.65 (ref. 47). Both these two facts make Shields *et al.* underestimate the snowball-melting stellar flux threshold. In comparison, the ice and snow albedos employed in our simulations are more reasonable.

Accuracy in low-temperature radiative transfer and snowball cloud simulations. Comparing with line-by-line radiative-transfer models, CAM3's radiative-transfer scheme is accurate for surface temperatures being equal to or less than 310 K (ref. 50). At 273 K, differences in longwave and shortwave radiation fluxes under clear-sky conditions between CAM3 and the two line-by-line radiative-transfer models are less than 5 W m^{-2}. The upper limit of CO_2 amount that CAM3 can simulate is ~100,000 ppmv (ref. 15). At this CO_2 level, differences in clear-sky outgoing longwave radiation between CAM3 and Kasting's radiative-transfer model[51] are within 2 W m^{-2}. We employ the solar spectrum and two stellar spectra corresponding to F-type (blackbody 7,200 K) and K-type (4,500 K) stars. Integrated broadband radiative flux difference[50] between a realistic spectrum and its corresponding blackbody spectrum is less than 7 W m^{-2}.

Through comparison with four state-of-the-art GCMs (CAM3, LMDz4, ECHAM6 and SP-CAM), a previous study[18] had established the fact that differences in net cloud radiative effect for Neoproterozoic snowball Earth simulations are within 10 W m^{-2} and differences in tropical and annual-mean surface temperature are within 5 K. Moreover, differences in the cloud radiative effect[19] between CAM3 and a cloud-resolving model (SAM) are within 2 W m^{-2}. These results imply that CAM3 is appropriate for simulating snowball clouds.

Combining the uncertainties in clear-sky and cloudy conditions, we state that the maximum uncertainty for simulating a snowball climate is within 17 W m^{-2}. This implies that the uncertainty range in estimating the stellar flux threshold for a snowball melting is ~170 W m^{-2} (that is, $4 \times 17/(1 - \alpha_p)$, where α_p is planetary albedo (such as 0.6) and the factor of 4 is the ratio of the planet's surface area to its cross-sectional area). This uncertainty is shown as a vertical bar in Fig. 2a.

Moist and runaway greenhouse limits. Both 1D radiative-transfer models and 3D GCMs have previously been employed to estimate the moist and runaway greenhouse limits. For a pure water vapour atmosphere and a surface albedo of 0.2, the runaway greenhouse limit under the solar spectrum is ~1,340 W m^{-2} in SMART[31] and ~1,420 W m^{-2} in the 1D radiative-transfer model LMDG[29] and Kasting's radiative-transfer model[30]. For an Earth-like atmosphere with saturated water vapour, the runaway greenhouse limit is ~1,430 W m^{-2} with an uncertainty range[50] of 10%. For an F-star spectrum, the moist and runaway greenhouse limits are higher, and for a K-star spectrum, the limits are lower[8,26,30].

The runaway greenhouse limit in the 3D GCM LMDG[29], ~1,500 W m^{-2}, is higher than in the 1D radiative-transfer model LMDG, mainly due to the effects of atmospheric sub-saturation. The moist greenhouse limit is ~1,430 W m^{-2} in ECHAM6 (ref. 28) and ~1,600 W m^{-2} in the GCMs CAM3 (ref. 26) and CAM_Wolf[27]. Divergences between the 3D GCMs are due to the differences in cloud parameterization[28] and shortwave absorption by water vapour[50].

A planet with weaker gravity has a lower runaway greenhouse limit than one with stronger gravity. On the basis of this, Pierrehumbert speculated that moons in Earth-like orbits are in either a runaway greenhouse state or a snowball state[12]. Note that moons as well as small planets are able to maintain long-lived and substantial atmospheres as long as their masses are greater than ~0.1–0.2 Earth's mass[52–55].

Climate transition simulations. In examining the post-snowball climate, CAM3 is coupled to a thermodynamic sea ice module[46] and to a 50-m slab ocean module[41]. Sea ice can grow and melt but glacier ice cannot in the model. Stellar flux is fixed to the typical stellar flux threshold for a snowball melting. No ocean heat transport has been included. The effects of stellar spectrum, planetary mass, CO_2 concentration and cloud particle size on the results are investigated; the post-snowball Earth climate that occurred ~600–800 million years ago is also examined (see Supplementary Table 2 and Supplementary Fig. 8). The experiments have an initial surface temperature of 250 K everywhere (a snowball state), and the time step is 60 s in the simulations using the standard version of the model and 10 s in the simulations using the modified version of the model that has a top pressure of 0.2 hPa. Each case is integrated for 80–120 model years.

Uncertainty in high-temperature radiative transfer. Comparing with line-by-line radiative-transfer models, CAM3 underestimates the greenhouse effect and shortwave absorption of water vapour at high temperatures[50], and the model crashes when the maximum surface temperature is higher than 340 K due to numerical instability and radiative-transfer limitation[56]. For example, at 320 K, the greenhouse effect and shortwave absorption in CAM3 is 8–11 W m^{-2} weaker than that in the two line-by-line models SMART and LBLRTM[50]. This implies that the surface temperature in the post-snowball state should be greater and stratospheric vapour concentration should be higher than those shown in Fig. 3 and Supplementary Fig. 3. Future simulations including high-temperature radiative transfer and H_2O photolysis are required to more precisely investigate the post-snowball climates.

Outgoing longwave radiation (OLR) curves and absorbed stellar radiation (ASR) values. At low temperatures, OLR is a nearly linear function of surface temperature, and at high temperatures, OLR asymptotes to a limiting, maximum value when the atmosphere becomes optically thick in all infrared wavelengths. Data for the OLR curves in Fig. 3f and Supplementary Fig. 9 are from Haqq-Misra *et al.*[57], and we have further included the effects of atmospheric sub-saturation[29,31] and clouds. This limiting OLR is approximately equal to the blackbody radiation corresponding to the temperature at the pressure level of one optical depth calculated down from the top of the atmosphere[12]. For pure water vapour, the limiting OLR[31] is ~282 W m^{-2}; for an atmosphere of 1-bar N_2 and saturated water vapour[29,31], it is ~292 W m^{-2}; the realistic atmosphere is sub-saturated and the limiting OLR would be higher, such as ~340 W m^{-2} if assuming relative humidity is 45%, close to the equivalent value in 3D GCMs[26,27]; clouds can decrease the limiting OLR by ~30 W m^{-2} (obtained in the CAM3 simulations of this work) through trapping infrared radiation from the surface. The limiting OLR for an atmosphere with 1-bar N_2, sub-saturated water vapour and clouds, therefore, is ~310 W m^{-2}.

The horizontal ASR lines in Fig. 3f are calculated on the basis of the stellar flux thresholds (2,100, 1,700 and 1,300 W m^{-2} for F, G and K stars, respectively) and planetary albedos (0.32, 0.24 and 0.34) from the last converged solution of CAM3 post-snowball experiments shown in Fig. 3a–e. The existence of a limiting OLR and ASR being larger than the limiting OLR are two necessary conditions for the onset of an unstable runaway greenhouse state[8,12].

Effects of atmospheric CO_2 on the stellar flux threshold and the post-snowball climate. How much atmospheric CO_2 could accumulate in a snowball state is determined by the balance between silicate (and seafloor) weathering and volcanic outgassing. To know the effect of CO_2 on the results, we perform five groups of experiments (Supplementary Fig. 6). When the surface albedo is set to 0.6 and CO_2 concentration is set to <3,000 ppmv, the snowball-melting stellar flux threshold is still higher than the runaway greenhouse limit[29]. This implies that the post-snowball planet will enter a runaway greenhouse state. If CO_2 concentration is

>3,000 ppmv, the post-snowball climate will be hot, but will not enter a runaway greenhouse state because the stellar flux threshold is lower than the runaway greenhouse limit. When the surface albedo is set to 0.8 for snow and 0.6 for sea ice and CO_2 concentration is <30,000 ppmv, a runaway greenhouse state after the snowball melting will also arise. But, if the CO_2 concentration is >30,000 ppmv, it will not.

An example of the post-snowball climate with a high concentration of CO_2, 100,000 ppmv, is shown in Supplementary Fig. 7. In this case, the snowball-melting stellar flux threshold is only ~1,360 W m^{-2}, the corresponding post-snowball global-mean surface temperature is 325 K, and stratospheric H_2O amount is lower than that required for entering a moist greenhouse state. However, the surface temperature and stratospheric H_2O amount are expected to decrease after the snowball deglaciation, because enhanced silicate weathering[58] following the melting would lead to the removal of atmospheric CO_2. Therefore, icy planets near the outer edge of the habitable zone that have an active carbon–silicate cycle may possess repeated climate cycles between the snowball state and the hot state[7,57]. This is different from the process of stellar brightening, in which the planet will enter a moist or runaway greenhouse state accompanying significant water loss from the ocean(s) and it has no chance to return back to a normal climate state.

A snowball Earth. The climate evolution associated with a snowball Earth 600–800 million years ago is summarized in Supplementary Fig. 8 (refs 4,16–18,59–66). As shown in the figure, the climate transition from the snowball Earth state to the post-snowball state is abrupt and dramatic, but the post-snowball state is in neither a moist greenhouse state nor a runaway greenhouse state. The reasons are as follows. First, the solar constant, 1,286 W m^{-2} (~6% fainter), is much lower than the runaway greenhouse limit[29] of ~1,500 W m^{-2}. Here we assume that atmospheric CO_2 concentration does not significantly influence the onset of a runaway greenhouse state[8]; this is because near the runaway greenhouse state H_2O becomes a major component of the atmosphere and dominates its infrared opacity. Second, after the snowball Earth melts, the surface is hot but the stratospheric H_2O mixing ratio is not higher than the moist greenhouse limit of 3×10^{-3}. This is due to the fact that CO_2 acts to warm the surface and troposphere but to cool the stratosphere and thereby decrease H_2O mixing ratio there[40]. Third, silicate weathering following the melting would enhance due to increased precipitation and runoff[58], which would lead to the removal of CO_2. The surface temperature and stratospheric H_2O amount are therefore expected to decrease after the hot period. The timescale of silicate weathering for dropping down the CO_2 concentration of ~100,000 ppmv to a normal level is ~10^6 years[58]. Even if assuming the stratospheric H_2O mixing ratio during the entire hot period were 3×10^{-3}, the loss of ocean water would be only 0.6 m, very tiny.

The climate evolution associated with early Mars and Venus can be inferred from the results for the snowball Earth. The solar constant on Mars is 591 W m^{-2}, and in the history it was lower. Thus, to melt a snowball Mars if it was, CO_2 concentration should be much higher than the CO_2 level for the snowball Earth melting. Due to the fact that CO_2 acts to cool the stratosphere, a post-snowball Mars would not enter a moist greenhouse state. A snowball Mars would also not transition to a runaway greenhouse state because its solar flux was much lower than the runaway greenhouse limit[12] of ~1,250 W m^{-2} under the Mars gravity of 3.71 m s^{-2}. Moreover, it is doubtful that Mars was ever in a snowball state. The current estimates for its initial global water inventory, <165 m global water equivalent[67], suggest that the planet was never as wet as Earth. Climate simulations show only about 30% of its surface was glaciated[68]. The solar constant on Venus is ~2,630 W m^{-2}, and in four billion years ago it was ~1,970 W m^{-2}. Both of these two insolation levels are higher than the stellar flux threshold for a snowball melting (Fig. 2a). This implies that it is unlikely that Venus had been in a snowball state.

Energy balance climate model. The climate transition and the effect of atmospheric greenhouse gas concentration on the transition can be further understood using a 0D energy balance climate model. The key processes of the model are ice-albedo feedback and water vapour feedback. Due to these two processes, there are multiple equilibrium states for a climate system (chapter 3 of ref. 12).

The balance between ASR and OLR determines the equilibrium surface temperature, as shown in Supplementary Fig. 9. In the figure, the ASR curves are calculated as $S_0/4 \times (1 - \alpha_p)$, where the albedo ($\alpha_p$) is 0.25 when the surface temperature is higher than 300 K and 0.60 when the surface temperature is lower than 260 K. Between the two temperatures, a quadratic interpolation[12] for the albedo is employed. For a relatively low stellar flux ($S_0 = 1,400$ W m^{-2}, the blue line in panel a), there are three solutions: a stable snowball state, an unstable partially ice-covered state, and a stable ice-free state. For a relatively high stellar flux ($S_0 = 1,700$ W m^{-2}, the red line in panel a), there are two solutions: a stable snowball state and an unstable partially ice-covered state. There is no equilibrium ice-free state for the case of $S_0 = 1,700$ W m^{-2}; as long as all of the surface ice melts, ASR would be higher than the allowed maximum OLR and the system would enter a runaway greenhouse state, which corresponds to the dramatic climate transition obtained in the 3D model CAM3.

If CO_2 concentration is high, the OLR curve shifts downward (Supplementary Fig. 9(b)), due to the CO_2 greenhouse effect. For the case of $S_0 = 1,400$ W m^{-2}, there are still three solutions but the two stable solutions (snowball and ice-free) are warmer than those in the case of a low CO_2 concentration. This is due to the CO_2 greenhouse effect. For the case of $S_0 = 1,700$ W m^{-2}, there is no equilibrium solution because the high CO_2 greenhouse effect prevents the system from staying in a snowball state, meanwhile the high stellar flux pushes the system into a runaway greenhouse state.

K and M stars. The abrupt climate transition does not apply to K- and M-star systems, due to their redder spectra and therefore lower ice/snow albedos and smaller snowball-melting stellar flux thresholds. Moreover, due to strong tidal forces, planets in the habitable zone of late K- and M-star systems are likely in spin–orbit resonance states[69], which has a profound impact on planetary climate[32]. A snowball planet in 1:1 resonance state (or called synchronous rotation) would require a much lower stellar flux to trigger the melting because all of the stellar energy is deposited on the permanent day side, compared with other resonance states.

Code availability. The code used to generate the data for this study are available in the PANGAEA repository, https://doi.pangaea.de/10.1594/PANGAEA.876224.

Data availability. The data that support the findings of this study are available in the PANGAEA repository, https://doi.pangaea.de/10.1594/PANGAEA.876224.

References

41. Collins, W. D. *et al*. *Description of the NCAR Community Atmosphere Model (CAM 3.0)* 214 (NCAR Tech. Note NCAR/TN-464+STR, 2004); http://www.cesm.ucar.edu/models/atm-cam/docs/description/description.pdf
42. Boville, B. A., Rasch, P. J., Hack, J. J. & McCaa, J. R. Representation of clouds and precipitation processes in the Community Atmosphere Model version 3 (CAM3). *J. Clim.* **19,** 2162–2183 (2006).
43. Abbot, D. S. & Pierrehumbert, R. T. Mudball: surface dust and snowball Earth deglaciation. *J. Geophys. Res.* **115,** D03104 (2010).
44. Abbot, D. S., Eisenman, I. & Pierrehumbert, R. T. The importance of ice vertical resolution for Snowball climate and deglaciation. *J. Clim.* **23,** 6100–6109 (2010).
45. Oleson, K. W. *et al*. *Technical Description of the Community Land Model (CLM)* 174 (NCAR Tech. Note NCAR/ TN-4611STR, 2004); http://opensky.ucar.edu/islandora/object/technotes:393
46. Briegleb, B. P. *et al*. *Scientific Description of the Sea Ice Component in the Community Climate System Model Version Three* 78 (NCAR Tech. Note NCAR/TN-463+STR, 2004); http://opensky.ucar.edu/islandora/object/technotes:391
47. Warren, S. G. & Brandt, R. E. Comment on "Snowball Earth: A thin-ice solution with flowing sea glaciers" by David Pollard and James F. Kasting. *J. Geophys. Res.* **111,** C09016 (2006).
48. Light, B., Brandt, R. E. & Warren, S. G. Hydrohalite in cold sea ice: laboratory observations of single crystals, surface accumulations, and migration rates under a temperature gradient, with application to "Snowball Earth". *J. Geophys. Res.* **114,** C07018 (2009).
49. Dadic, R. *et al*. Effects of bubbles, cracks, and volcanic tephra on the spectral albedo of bare ice near the Transantarctic Mountains: implications for sea glaciers on Snowball Earth. *J. Geophys. Res.* **118,** 1658–1676 (2013).
50. Yang, J. *et al*. Differences in water vapor radiative transfer among 1D models can significantly affect the inner edge of the habitable zone. *Astrophys. J.* **826,** 222 (2016).
51. Kasting, J. F. & Ackerman, T. P. Climatic consequences of very high CO_2 levels in Earth's early atmosphere. *Science* **234,** 1383–1385 (1986).
52. Williams, D. M., Kasting, J. F. & Wade, R. A. Habitable moons around extrasolar giant planets. *Nature* **385,** 234–236 (1997).
53. Lammer, H. *et al*. Origin and stability of exomoon atmospheres: implications for habitability. *Orig. Life Evol. Biosph.* **44,** 239–260 (2014).
54. Kipping, D. M., Bakos, G. À., Buchhave, L., Nesvorny, D. & Schmitt, A. The hunt for exomoons with Kepler (HEK). I. Description of a new observational project. *Astrophys. J.* **750,** 1–19 (2012).
55. Heller, R. *et al*. Formation, habitability, and detection of extrasolar moons. *Astrobiology* **14,** 798–835 (2014).
56. Kopparapu, R. K. *et al*. The inner edge of the habitable zone for synchronously rotating planets around low-mass stars using general circulation models. *Astrophys. J.* **819,** 1–14 (2016).
57. Haqq-Misra, J., Kopparapu, R. K., Batalha, N. E. & Kasting, J. Limit cycles can reduce the width of the habitable zone. *Astrophys. J.* **827,** 1–10 (2016).
58. Le Hir, G. *et al*. The snowball Earth aftermath: exploring the limits of continental weathering processes. *Earth Planet. Sci. Lett.* **277,** 453–463 (2008).

59. Yang, J., Peltier, W. R. & Hu, Y. The initiation of modern "soft snowball" and "hard snowball" climates in CCSM3. Part I: the influences of solar luminosity, CO_2 concentration, and the sea ice/snow albedo parameterization. *J. Clim.* **25,** 2711–2736 (2012).

60. Yang, J., Peltier, W. R. & Hu, Y. The initiation of modern "soft snowball" and "hard snowball" climates in CCSM3. Part II: climate dynamic feedbacks. *J. Clim.* **25,** 2737–2754 (2012).

61. Yang, J., Peltier, W. R. & Hu, Y. The initiation of modern soft and hard Snowball Earth climates in CCSM4. *Clim. Past* **8,** 907–918 (2012).

62. Liu, Y., Peltier, W. R., Yang, J. & Vettoretti, G. The initiation of Neoproterozoic "snowball" climates in CCSM3: the influence of paleocontinental configuration. *Clim. Past* **9,** 2555–2577 (2013).

63. Liu, Y., Peltier, W. R., Yang, J., Vettoretti, G. & Wang, Y. Strong effects of tropical ice sheet coverage and thickness on the hard snowball Earth bifurcation point. *Clim. Dynam.* **48,** 3459–3474 (2016).

64. Hyde, W. T., Crowley, T. J., Baum, S. K. & Peltier, W. R. Neoproterozoic 'snowball Earth' simulations with a coupled climate/ice-sheet model. *Nature* **405,** 425–429 (2000).

65. Peltier, W. R., Liu, Y. & Crowley, J. W. Snowball Earth prevention by dissolved organic carbon remineralization. *Nature* **450,** 813–818 (2007).

66. Liu, Y. & Peltier, W. R. A coupled carbon cycle-climate model of neoproterozoic glaciation: influence of continental configuration on the formation of a "soft snowball". *J. Geophys. Res.* **115,** D17111 (2010).

67. Villanueva, G. L. *et al.* Strong water isotopic anomalies in the Martian atmosphere: probing current and ancient reservoirs. *Science* **348,** 218–221 (2015).

68. Wordsworth, R. *et al.* Global modelling of the early Martian climate under a denser CO_2 atmosphere: water cycle and ice evolution. *Icarus* **222,** 1–19 (2013).

69. Leconte, J., Wu, H., Menou, K. & Murray, N. Asynchronous rotation of Earth-mass planets in the habitable zone of lower mass stars. *Science* **347,** 632–635 (2015).